Fatigue Fract. Engng Mater. Struct. Vol. 17, No. 6, pp. 695–707, 1994
Printed in Great Britain.

8756-758X/94 $6.00 + 0.00

ANALYZING DUCTILE FRACTURE USING DUAL DILATIONAL CONSTITUTIVE EQUATIONS

Z. L. ZHANG and E. NIEMI
Department of Mechanical Engineering, Lappeenranta University of Technology, P.O. Box 20, FIN-53851 Lappeenranta, Finland

Received in final form 25 February 1994

Abstract—By adopting a suggestion made by Thomason, a new failure criterion for the Gurson–Tvergaard model has been recently introduced by the authors. In this study, a method based on the Gurson–Tvergaard constitutive model and the new failure criterion is applied to the analysis of ductile fracture. The main features of the method are that the material failure is a natural process of the development of Thomason's dual dilational constitutive responses, and the void volume fraction corresponding to the failure by void coalescence is not necessarily a material constant and is not needed to be fitted beforehand. Furthermore, void nucleation parameter(s) can be numerically fitted from experimental tension results. This method has been implemented into the ABAQUS finite element program via a user material subroutine and is applied to the prediction of tension problems conducted by the authors. In the analyses, two strain-controlled void nucleation models have been studied and compared. The void nucleation parameters corresponding to the two models have been calibrated. The crack initiation of both smooth and notched axisymmetric tensile specimens are well predicted by the method. Finally, several critical issues in the analysis of ductile fracture are discussed.

INTRODUCTION

It is known that ductile fracture occurs in plastic deforming metals through the nucleation, growth and coalescence of small voids or cavities. Considerable effort has been expended in the past two decades in the development of ductile fracture characterization of engineering materials; such as J-integral, COD, etc. However, applications of these criteria addressed to the whole history and the fracture from the initiation to rapid crack growth have caused concern when large irreversible plastic deformation is developed at the crack tip. Due to the limitations of the conventional global fracture criteria, there has recently been considerable interest and research on "local approaches" to fracture [1–5].

A micro-mechanical model based yield function introduced by Gurson [6,7] and modified by Tvergaard [8,9] has been applied more than any other models as a dilational constitutive equation. In the Gurson–Tvergaard model, the void volume fraction of the material has been incorporated into the yield function. Although the Gurson–Tvergaard model, therefore, demonstrates the softening effect of the material, the model itself does not constitute a fracture criterion. Hence, a criterion for void coalescence has to be used to simulate the material failure.

In line with pure mathematical convenience, a criterion (Fc) using a constant critical void volume fraction, f_c, has almost always been used in theoretical analyses and practical applications using the Gurson–Tvergaard model [10–15]. However, whether the critical void volume fraction is a material constant, or whether the critical void volume fraction is independent of the stress state, is questionable. On the other hand, the constant critical void volume fraction is difficult to determine and there is a possible discrepancy in Fc when the void nucleation is taken into account. A detailed discussion of this problem will be presented in the next section.

Recently, based on a proposal made by Thomason [16] and by modifying Thomason's plastic limit–load criterion (Sc) [16–18] for void coalescence, a new failure criterion (NSc) which is fully compatible with the Gurson–Tvergaard model has been introduced by the authors [19]. The criterion is a natural result of the development of dual, stable and unstable, constitutive responses introduced by Thomason [16,17]. According to Thomason's theory [16,17], in the beginning of plastic loading, the deformation is homogeneous and the material is controlled by the stable dilational constitutive response. During the loading, once the unstable dilational response, which signifies the void coalescence mode, prevails, then the material starts to fail.

In this study, the Gruson–Tvergaard model and the new failure criterion have been implemented into the commercial finite element program ABAQUS via the user material subroutine. This method is applied to the analysis of ductile fracture of tension specimens tested by the authors. It will be shown that this method can well predict the crack initiation and fracture behaviour of smooth and notched axisymmetric tensile specimens. The main features of this method are that the critical void volume fraction, f_c, which signifies the material failure by void coalescence need not be predetermined. On the other hand, the void nucleation parameter(s) which is difficult to monitor in experiments and is usually "arbitrarily" chosen, can be numerically calibrated from, for example, notched axisymmetric tension tests. The final purpose of our studies is to simulate the ductile fracture behaviour of welded T-joints by using this method. The parameters calibrated from this study together with the parameters for heat-affected-zone (HAZ) material will be used in the analysis of welded joints.

GURSON–TVERGAARD MODEL AND ITS FAILURE CRITERIA

Gurson–Tvergaard model

The Gurson–Tvergaard model [6–9] has recently been increasingly popular for simulating plastic flow localization and ductile fracture problems. A detailed description of the model can be seen in [6,9]. In the following text only a brief overview of the model is provided.

Gurson [6,7] proposed the following approximate yield function ($q_1 = 1$, $q_2 = 1$) for a porous solid with a randomly distributed volume fraction f of voids:

$$\phi(\sigma, f, \bar{\sigma}) = \frac{q^2}{\bar{\sigma}^2} + 2q_1 f \cosh\left(\frac{3q_2\sigma_m}{2\bar{\sigma}}\right) - 1 - (q_1 f)^2 = 0 \tag{1}$$

where constants q_1 and q_2 were introduced by Tvergaard [8,9] to bring predictions of the model into closer agreement with full numerical analyses of a periodic array of voids. Here σ_m and q are the mean normal and effective part of the average macroscopic Cauchy stress $\boldsymbol{\sigma}$, and $\bar{\sigma}$ is the yield stress of the matrix material. The void volume fraction increase in the model is written:

$$df = df_{\text{growth}} + df_{\text{nucleation}} \tag{2}$$

The void growth law is described by:

$$df_{\text{growth}} = (1 - f)d\boldsymbol{\varepsilon}^p : \boldsymbol{I} \tag{3}$$

which is an outcome of plastic incompressibility of the matrix material. In Eq. (3), $d\boldsymbol{\varepsilon}^p$ and $\boldsymbol{I}$ are the plastic strain increment tensor and the second order unit tensor, respectively. In reality, void nucleation is a very complicated and difficult matter. Nevertheless, the nucleation of new voids in the Gurson–Tvergaard model is usually taken to be either strain-controlled or stress-controlled [6]. Because they are relatively easy to handle, strain-controlled nucleation models are widely

used in the literature [8,9,13–15]

$$df_{\text{nucleation}} = Ad\bar{\varepsilon}^{\text{P}} \tag{4}$$

where $\bar{\varepsilon}^{\text{P}}$ is the equivalent plastic strain in the matrix material. Parameter A depends on the void nucleation model used. Two strain-controlled void nucleation models have been seen in the literature. One is the continuous nucleation model by Gurland [20] with a linear relation to equivalent plastic strain (A is kept constant). Another one was proposed by Chu and Needleman [21] where the void nucleation is assumed to follow a normal distribution as suggested:

$$A_1 = \frac{f_{\text{N}}}{S_{\text{N}}\sqrt{2\pi}} \exp\left[-\frac{1}{2}\left(\frac{\bar{\varepsilon}^{\text{P}} - \varepsilon_{\text{N}}}{S_{\text{N}}}\right)^2 \right] \tag{5}$$

with f_{N} = volume fraction of void nucleating particles, ε_{N} = mean strain for void nucleation, S_{N} = corresponding standard deviation. In general, for the strain-controlled nucleation case, the coefficient A in Eq. (4) can be written

$$A = A_0 + A_1 \tag{6}$$

where A_0 is the constant or void nucleation intensity of the continuous void nucleation model.

Furthermore, the equivalence of the overall rate of plastic work and that in the matrix material leads to

$$\boldsymbol{\sigma} : d\boldsymbol{\varepsilon}^{\text{P}} = (1-f)\bar{\sigma} d\bar{\varepsilon}^{\text{P}}. \tag{7}$$

The flow rule is usually assumed to obey macroscopic normality, so that,

$$\varepsilon_{\text{ij}}'^{\text{P}} = \lambda' \frac{\partial \phi}{\partial \sigma_{\text{ij}}}. \tag{8}$$

It can be easily seen that the Gurson–Tvergaard model itself does not constitute any fracture criterion. An extra failure criterion should be used to signify the material failure by void coalescence. Once the failure by void coalescence appears according to a specific criterion, numerically it is preferred to simulate the material separation gradually, rather than suddenly. Therefore, a modification using the following f^* to replace f in Eq. (1) has been proposed by Tvergaard and Needleman [10] and applied in our study:

$$f^* = \begin{cases} f & \text{for } f \leqslant f_{\text{c}} \\ f_{\text{c}} + K(f - f_{\text{c}}) & \text{for } f > f_{\text{c}} \end{cases}. \tag{9}$$

Here, f_{c} is the critical void volume fraction at which voids coalesce, which in the present study was determined by the new criterion, and K is a constant determined from the void volume fraction, f_{F}, which is the void volume fraction at final failure of the material:

$$K = \frac{f_{\text{u}}^* - f_{\text{c}}}{f_{\text{F}} - f_{\text{c}}} \tag{10}$$

where f_{u}^* is the ultimate void volume fraction and $f_{\text{u}}^* = 1/q_1$.

Failure criteria

Two failure criteria, namely Fc and Sc for the Gurson–Tvergaard model have been identified by the authors [19,22,23]. Here Fc is the criterion using a constant critical void volume fraction f_{c}, which can be either determined by a cell model analysis [24] or by a method proposed by Sun

et al. [14,15]. Here, "constant" means that the critical void volume fraction is independent of stress triaxiality and can be applied to other stress states, once determined from one stress state. It has been pointed out [19,22] that even in the absence of void nucleation, f_c is difficult to determine. When void nucleation is taken into account, f_c depends on the choice of the nucleation parameter(s). Because of the difficulty in measuring the nucleation parameter(s) in practice, usually an approximate void nucleation model and parameter(s) are used. There is a possible discrepancy in Fc when void nucleation is considered, which can be illustrated in the following simple numerical example. In the numerical example, two pairs of parameters were used: case 1, $f_0 = 0.0$, $f_N = 0.04$, $\varepsilon_N = 0.3$ and the calibrated $f_c = 0.104$; case 2, $f_0 = 0.0$, $f_N = 0.04$, $\varepsilon_N = 0.25$ and the calibrated $f_c = 0.109$. In these two pairs, there is only a slight difference in ε_N. Case 1 was probably first used in [10] and lately widely used in the literature.

The two f_c values were calibrated from a smooth axisymmetric tensile specimen which is approximately simulated by one element with stress triaxility $T = 0.333$ (T is defined as the ratio of σ_m/q) and stopped at axial strain 1.2. A power-hardening matrix material with power 0.11 was used in the numerical example. Figure 1(a) shows that the two pairs of parameters give virtually identical predictions but different critical void volume fractions. Then these two pairs of parameters were applied to a high stress triaxility ($T = 2$) case. It can be found that there are considerable differences both in the ductility and load-carrying behaviour, see Fig. 1(b). Therefore, the non-unique nature of Fc would in certain cases yield large differences in practical applications. Here we only slightly changed the value of ε_N; similarly or possibly even worse behaviour may be expected if other parameter(s) are varied.

Thomason [16–18] has developed a dual dilational–plastic response theory for ductile fracture by void coalescence. According to his theory, Thomason [16] has also suggested two modifications to the Gurson–Tvergaard model. Based on one of the suggestions and by modifying Thomason's [16] micro-mechanical plastic limit–load model for void coalescence (Sc), a new failure criterion (NSc), for the Gurson–Tvergaard model has been recently introduced by the authors [19,22]. In Sc and NSc, ductile fracture is interpreted as an unstable bifurcation of the macroscopic plastic flow field in the model bulk material. This bifurcation is the transition from a homogeneous flow field to one in which deformation is concentrated in a thin band. Two dilational yield surfaces have been defined by Thomason [16]. They are: the weak dilational yield surface, which represents the stable homogeneous plastic flow field, and the strong dilational surface, which signifies the virtual unstable mode of incipient void coalescence. Thomason [16] observed that a necessary condition for continuing homogeneous ductile flow in a 2D void-containing body (see Fig. 2(a)) is that the virtual mode of incipient void coalescence cannot develop in the intervoid matrix,

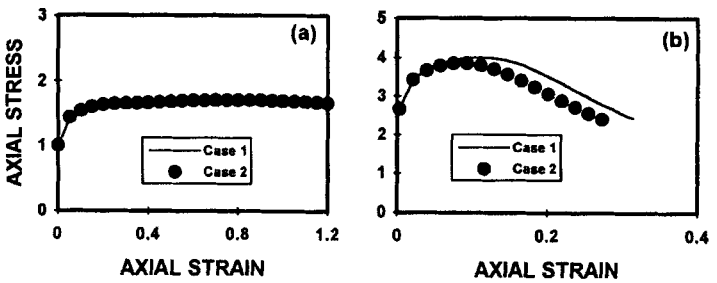

Fig. 1. Normalized stress–strain in axial direction for the case with stress triaxiality (a) $T = 0.333$, (b) $T = 2.0$.

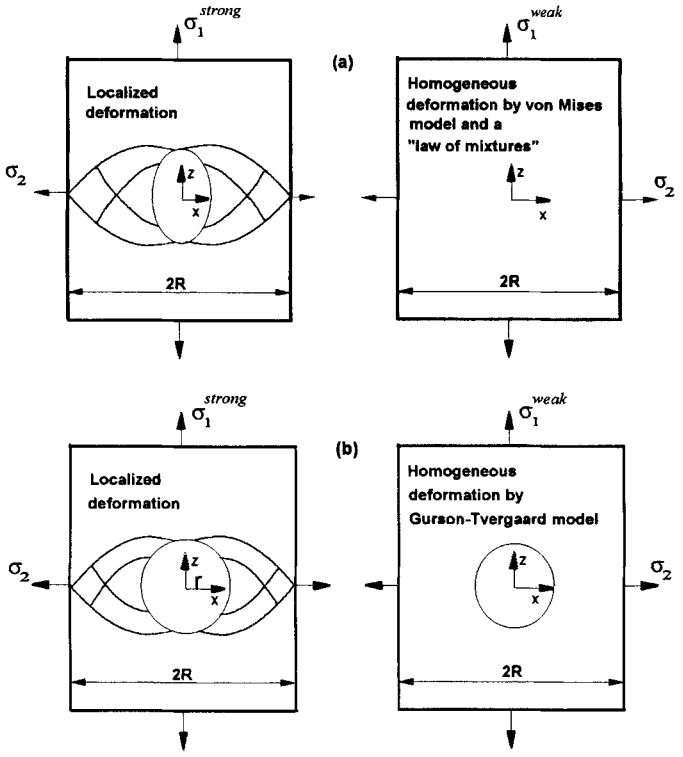

Fig. 2. Dual dilational 2D constitutive responses (a) the original, introduced by Thomason [16,17] and (b) the modified responses in this study.

$\sigma_1^{\text{weak}} < \sigma_1^{\text{strong}}$. Therefore, the critical condition for the failure by void coalescence can be written:

$$\sigma_1^{\text{weak}} = \sigma_1^{\text{strong}} \tag{11}$$

where σ_1^{weak} is the current maximum principal stress for the homogeneous flow field on the weak dilational–plastic yield surface, which for a real problem can be calculated by any analytical or numerical method, eg. the finite element method; and σ_1^{strong} is the incipient void coalescence stress on the strong dilational–plastic yield surface [16] which is directly related to the plastic constraint factor by:

$$\sigma_1^{\text{strong}} = \frac{\sigma_n}{\bar{\sigma}} A_n \bar{\sigma} \tag{12}$$

where $\sigma_n/\bar{\sigma}$ is the plastic constraint factor presented by Thomason [16] and A_n is the net area fraction of intervoid matrix in the maximum principal stress direction which in this case is the z direction (Fig. 2). It must be noted that σ_1^{weak} depends on the material model adopted, current stress state and internal state variables, while σ_1^{strong} is solely determined by the current void–matrix dimensions and the yield stress of the matrix material.

The original plastic limit–load model [16] was based on the void shape (elliptical) calculated using the Rice–Tracy theory [25] and real void-matrix dimensions. Furthermore, von Mises yield model was adopted as the weak dilational yield surface. The macroscopic yield stress was approximately decreased using a "law of mixtures" [16] to consider the dilational effect caused by the

void. With these limitations in mind, the following modifications have been tested by the authors [19,23]: as originally suggested by Thomason [16], use the Gurson–Tvergaard model to characterize the material as the weak yield surface; furthermore, assume that the void grows *spherically* and calculate the void and matrix geometry changes using the current strain and void volume fraction from the Gurson–Tvergaard model. These modifications, illustrated in Fig. 2(b), lead to a new failure criterion [19,22] which is fully compatible with the Gurson–Tvergaard model. By comparing the predictions by the new failure criterion with the finite element results of Koplik and Needleman [24], the authors [19,22] concluded that the new failure criterion is not only accurate, but also versatile. According to these modifications, the void–matrix geometry for the 2D problem shown in Fig. 2(b) can be calculated:

$$r = \sqrt{\frac{f}{\pi} e^{\varepsilon_x + \varepsilon_z}} \tag{13}$$

$$R = R_0 \varepsilon^{\varepsilon_x} \tag{14}$$

where ε_x and ε_z are the strains in x and z axes, R_0 is the initial value of R and f is the current void volume fraction. After the modification, the plastic constraint factor is solely determined by r/R as

$$\frac{\sigma_n}{\bar{\sigma}} A_n = g\left(\frac{r}{R}\right) = \frac{0.3}{r/(R-r)} + 0.6 \tag{15}$$

for the plane strain problem. Equation (15) was presented by Thomason [16] and is derived from plane-strain slip–line field solutions for the microvoid coalescence problem.

Then the plastic limit–load condition, Eq. (11), after modification can be rewritten as:

$$g\left(\frac{r}{R}\right) = \frac{\sigma^{\text{weak}}}{\bar{\sigma}}. \tag{16}$$

With Eqs (13), (14) and the maximum principal stress which can be calculated from the Gurson–Tvergaard model, the plastic limit–load condition Eq. (16) can be evaluated. Once the condition is satisfied, the void coalescence starts to occur and the void volume fraction at this point is the critical void volume fraction, f_c, in the Gurson–Tvergaard model.

The above work makes the plastic limit–load model fully compatible with the Gurson–Tvergaard model, such that no extra work is necessary, except the evaluation of the void coalescence condition. From Eqs (13) and (14), it can be seen that the left hand side of Eq. (16) is a function of f, ε_x and ε_z.

NUMERICAL PROCEDURES

The method described above has been incorporated into the ABAQUS program, via the user material subroutine. The non-linear equations were solved using the Newton method. The numerical integration was efficiently performed using the generalized mid-point algorithms and their explicit seven-constant consistent tangent moduli for pressure-dependent material models recently developed by the authors [22,26,27]. It has been found that for the Gurson–Tvergaard model, the true mid-point algorithm is usually the most accurate one, and the one-step Euler forward algorithm has the poorest accuracy. However, considering the extra non-symmetric property of consistent tangent moduli of the true mid-point algorithm, in general the Euler backward algorithm is recommended [22,27]. The following sequence is used in the method. First in the user subroutine, the stress was updated using the Euler backward algorithm [20,27]. During the stress updating,

the maximum principal stress and strains are evaluated. After the stress has been updated, the plastic limit–load constraint factor was calculated and compared with the maximum principal stress to test the void coalescence condition. Once the failure condition is satisfied, the modification to take into account the void coalescence effect, Eq. (9), is used. Finally, the linearization or consistent tangent moduli is obtained. It should be noted that the value of the ultimate void volume fraction f_u^* has no physical meaning but the product $q_1 f_u^*$ in the yield function may not equal to 1, in order to keep numerical stability. For this reason, $q_1 f_u^* \approx 0.9$ was used.

APPLICATIONS

In order to test the present method and obtain the necessary parameters for the simulation of welded T-joints, axial tensile specimens were tested by the authors, which included smooth and notched specimens. The experiments were performed with a Finnish steel, Fe510. The main elements of the chemical composition (wt.%) of the steel were: 0.136 C, 1.47 Mn, 0.15 Si, 0.0065 S and 0.016 P.

A wide series of tests for (cold-formed) rectangular hollow section K-joints have been performed [28]. This study is one step in an attempt to explain the fracture behaviour of these specimens. Because raw material was not available, the material of the tensile specimens was cut from an undeformed area of the cold-formed rectangular hollow section chords (made of hot-rolled plate) of the joint specimens. The nominal thickness of the hollow section is 8 mm. The diameter of the smooth bar and maximum and minimum diameters of the notched ones are 4, 7 and 4 mm, respectively. Two notch radii, 1.75 (mesh AX1) and 0.875 (mesh AX2) mm were used. The finite element meshes for the smooth (AX0) and two notched specimens are shown in Fig. 3. In order to test the mesh size effect, very fine meshes for the two notched specimens were created, with one for notched specimen 1, shown in Fig. 3, for comparison purposes. An initial imperfection of 0.01 mm in diameter was used at the bottom of model AX0 in order to initiate the necking. An important step in the analysis of a smooth bar is the simulation of the necking which usually occurs at maximum load during the displacement-controlled test [15]. It has been shown by many researchers that the Bridgman approach [16,29] can well calibrate the true stress–strain relation. The Bridgman-corrected true stress–strain relation of the present material was used in all the analyses. The elastic parameters used were Young's modulus $E = 206$ GPa and Poisson's ratio 0.3. The initial yield stress of the steel was 480 MPa. Below 0.195 strain, the true stress – true strain was approximated by multi-linear curves. No hardening was available after a strain of 0.5. Between 0.195 and 0.5, an extrapolation $\bar{\sigma} = 685\bar{\varepsilon}^{0.085}$ was used. In the following analysis, $f_F = 0.125$ and

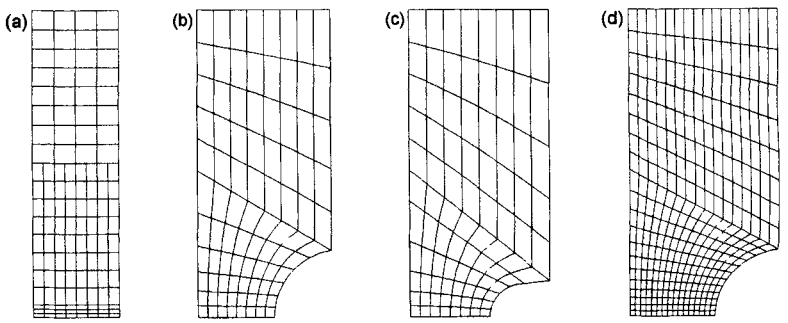

Fig. 3. Axisymmetric finite element meshes for smooth and notched specimens, (a) AX0, (b) AX1, (c) AX2 and (d) FAX1.

$f_u^* = 0.605$ in Eq. (10) were used, except for the cases otherwise mentioned. As proposed by Tvergaard [8,9], $q_1 = 1.5$ and $q_2 = 1.0$ were used in Eq. (1).

The main chemical composition of the steel is similar to the steel in [30]. A metallographic analysis of the inclusions, mainly manganese sulphides, gave the average size in the length direction of 5.7 μm, with minimum size 2.8 μm and maximum 42.5 μm. The metallographic data for the area or volume fraction of the inclusions was not available. However, the inclusion dimensions of present material is very close to those of the material studied in [3]. Both Refs [30] and [3], where metallographic data for inclusion volume fraction was available, have shown that an approximate formula by Franklin [31] can well estimate the volume fraction of MnS inclusions. So, as a first approximation, the initial void volume fraction is taken to be the volume fraction of MnS inclusions [3,30] estimated from the formula by Franklin [31]

$$f_v = 0.054\left(\mathrm{S}(\%) - \frac{0.001}{\mathrm{Mn}(\%)}\right)$$

For the present steel S = 0.0065% and Mn = 1.47% and so $f_0 = f_v = 0.00031$, which is reasonable compared with values given in [3,14,15,30]. As is normal practice, the initial void volume fraction is assumed to be present at the beginning of plastic loading. This initial void volume fraction f_0, has been applied in all the analyses of the specimens, with results shown in Fig. 4. It has been clearly shown that with f_0 alone, the predicted diameter-reductions corresponding to crack in-

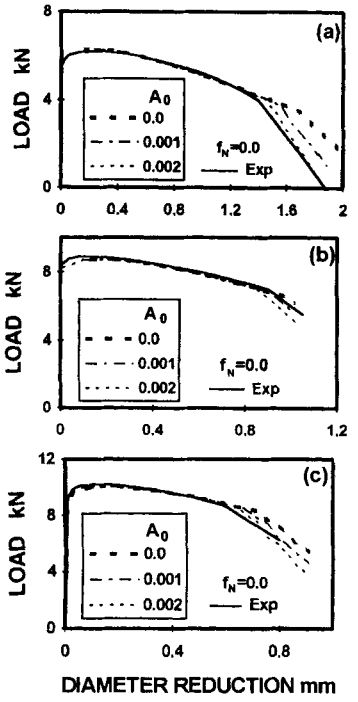

Fig. 4. Load-diameter reduction curves of (a) smooth specimen, mesh AX0, (b) notched specimen 1, mesh AX1 and (c) notched specimen 2, mesh AX2. The continuous void nucleation model was used in the calculation.

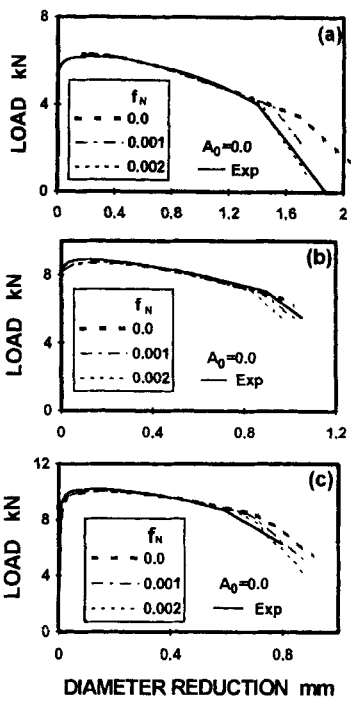

Fig. 5. Load-diameter reduction curves of (a) smooth specimen, mesh AX0, (b) notched specimen 1, mesh AX1 and (c) notched specimen 2, mesh AX2. The void nucleation model by Chu and Needleman [21] was used in the calculation.

itiation are too large compared with the experimental ones in all the three cases. Therefore, it means the nucleation of new voids during the loading should be taken into account in the analyses. The two void nucleation models introduced early were tested. The typical shapes of the two models are shown in Fig. 6. As described before, one main feature of the present method is that the critical void volume fraction does not need to be determined beforehand and the nucleation parameters A_0 or A_1 can be fitted from experimental results. In the following, we shall try to fit the void nucleation parameters.

At first, the continuous void nucleation model was adopted. Three values of A_0, 0.0, 0.001 and 0.002 were tested. The predicted results are compared with experimental ones for the three specimens in Fig. 4. It can be seen that the difference in crack initiation caused by the difference in A_0 is larger for the smooth specimen than for the notched specimens. On average, the value $A_0 = 0.002$ gives the best predictions for the three cases.

Then the void nucleation model by Chu and Needleman [21] with $\varepsilon_N = 0.3$ and $S_N = 0.1$ was tried. Also three values of f_N, 0.0, 0.001 and 0.002 were tested. The predicted results are shown in Fig. 5. Although the nucleation intensity of this model is very different to that of the continuous model (see Fig. 6), it is interesting to find that the predictions by this model are quite similar to those by the continuous model. As in the continuous model, the value 0.002 for f_N generally gives the best fit to the experimental results.

DISCUSSION

Void nucleation modelling

There are two kinds of void nucleation in the Gurson–Tvergaard model: the initial void nucleation of large inclusions and the intermediate void nucleation of secondary particles or small carbides. As mentioned earlier, in line with convenience, it is usually assumed that the initial voids nucleate at the beginning of plastic deformation, although nothing prohibits the introduction of a nucleation criterion for the initial voids. It has been shown that the modelling of intermediate nucleation is necessary and important in the analysis using the Gurson–Tvergaard model, at least for this steel. The use of the strain-controlled nucleation model has several advantages, it is easy to handle and no extra term added to the asymmetry of the tangent moduli. In practice, it is very difficult to determine the void nucleation model and its parameters. In failure criterion Fc, the nucleation parameter(s) is usually selected beforehand and the critical void volume fraction is determined later, or vice versa. Because there is no mechanism for void coalescence available in Fc, for any strain-controlled nucleation model, either the nucleation parameter(s) or the critical

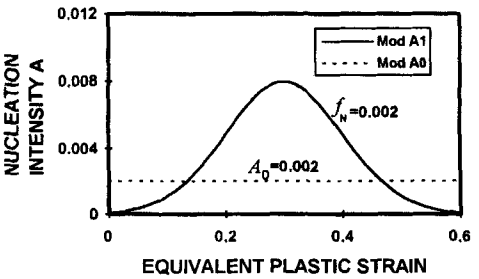

Fig. 6. Void nucleation intensities as a function of equivalent plastic strain for two void nucleation models. Mod A0 is the continuous void nucleation model and Mod A1 denotes the void nucleation model by Chu and Needleman [21].

void volume fraction can be taken as independent variables. Thus the non-consistency problem described earlier occurs in Fc. However, in the new criterion NSc, a coalescence mechanism which is fully compatible with the Gurson–Tvergaard model has been installed into the Gurson–Tvergaard model. Void coalescence is therefore a natural development of the stable and unstable responses. In contrast with Fc, in NSc the void nucleation parameter(s) is the only independent variable which can be fitted from experimental results. In nature, the discrepancy problem has not been absolutely eliminated in NSc, because of the inability to determine accurately the void nucleation model and select its parameters, for example, the values of ε_N and S_N. However, for a simple nucleation model such as the continuous void nucleation model, the nucleation parameter is solely determined without any ambiguity. Two nucleation models have been compared in the previous section. It was interesting to find that the simple continuous nucleation model works equally as well as the more complicated model by Chu and Needleman [21]. This finding may suggest that by using the simple nucleation model and the new failure criterion, the risk of a non-consistency problem could be reduced to as small as possible.

Effect of mesh size

One of the important aspects in continuum damage mechanics is the so-called critical length effect. Because the finite element method is usually involved in continuum damage mechanics, so the critical length is directly related to the finite element mesh size. It is essential to note that the mesh size effect is effective only when the stress distribution is uneven. Two meshes, FAX1 (shown in Fig. 3) and FAX2 which use half of the mesh size of AX1 and AX2 were created in order to study the mesh size effect. Figure 7 shows the stress triaxiality results near the minimum section at the nearest integration point to the centre and at the nearest integration point to the surface as a function of the macroscopic equivalent strain, $2\ln(D_0/D_1)$, where D_0 and D_1 are the initial and current diameter at the notch. It should be mentioned that in Fig. 7, von Mises yield model was used. It can be seen that in both cases studied the mesh size has negligible effect on the stress triaxiality, especially at the centre. As well as the mesh size effect on stress triaxiality, the effect on the fracture behaviour has also been studied, which is shown in Fig. 8. It can be observed that crack initiation in the fine mesh, FAX1, occurred slightly earlier than that in AX1. The only significant effect of the mesh size is the post initiation load diameter-reduction behaviour, which is not very important in the calibration of nucleation parameters. A similar finding has been reported by Batisse *et al.* [30]. In conclusion, the mesh size effect in the notched tension specimens studied is not significant and the finite element meshes used in this study are accurate enough for

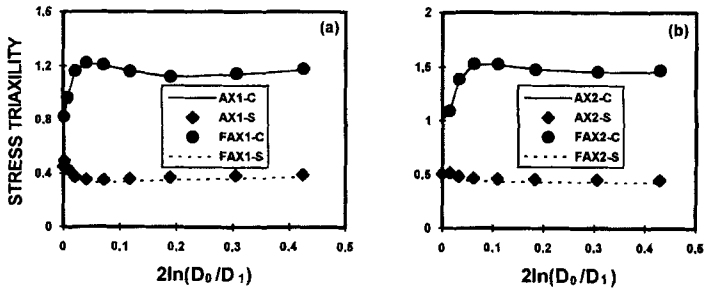

Fig. 7. Stress triaxility as a function of the macroscopic equivalent strain for (a) notched specimen 1 and (b) notched specimen 2. No damage is involved in the calculation. In the legend "-c" means the centre and "-s" the surface.

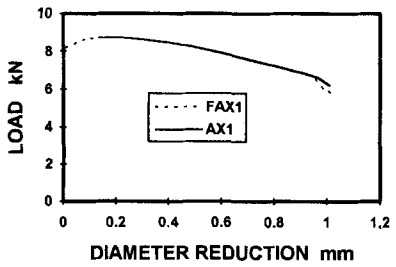

Fig. 8. Load-diameter reduction curves of notched specimen 1, mesh AX1 and FAX1, $A_0 = 0$, $f_N = 0$, $f_0 = 0.00031$.

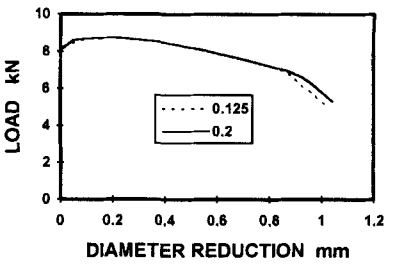

Fig. 9. The effect of f_F, mesh AX1, $A_0 = 0.002$, $f_N = 0$. The values in the legend are for f_F.

void nucleation fitting. In other words, stress distribution in the notched specimens is smooth enough so that the effect of mesh size on the void nucleation parameters to be calibrated may be neglected.

Effect of f_F

The parameter f_F in Eq. (9) is defined as the void volume fraction at final failure of the material, which could be obtained from experiment. The value of 0.25 was originally suggested by Tvergaard and Needleman [10] and has been widely used since then. As stated earlier the value 0.125 was used in the previous analyses. Another value of 0.2 was also tested in one analysis for comparison, which is shown in Fig. 9. Figure 9 clearly indicates that f_F will affect the post initiation load diameter-reduction behaviour, the smaller the f_F value, the faster the load decreases.

2D and 3D failure criteria

It should be mentioned that in this study a 2D plane strain failure criterion has been applied to the analysis of an axisymmetric fracture problem. Strictly speaking this is an approximation. The situation is similar to the Gurson model. The original Gurson model was constructed from a 2D plane strain yield field where a cylindrical void was assumed and a 3D yield field which contains a spherical void. Nevertheless, the Gurson model has been widely applied to axisymmetric problems, where axisymmetric voids by nature are involved. In order to assess the validity of a 2D criterion on axisymmetric problems, the 3D criterion [19] has also been applied in one case. The results using a 3D criterion is compared with the results using a 2D criterion in Fig. 10. The comparison shows that the initiations predicted by 2D and 3D criteria are in very close agreement, with 3D criterion predicting a slightly later crack initiation. Thomason [16] has compared the

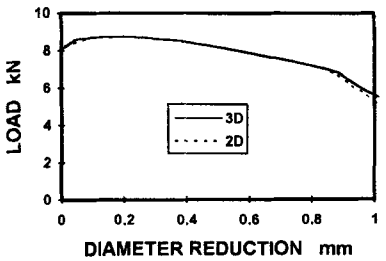

Fig. 10. Predictions using 2D and 3D failure criteria, mesh AX1, $A_0 = 0.002$, $f_N = 0$, $f_F = 0.125$, $f_0 = 0.00031$.

critical void growth strains from his original 2D and 3D ductile fracture criteria. For the same initial void volume fraction, he found that the critical "limit load" stress by 2D and 3D criteria were quite close to each other, even though the intervoid matrix geometries of the 2D and 3D models differ substantially. The actual solution for the axisymmetric problem must be near or between the 2D and 3D solution, so the above findings suggest that 2D or 3D criterion may be used for an axisymmetric problem as a first approximation.

SUMMARY

A method using dual dilational constitutive responses has been applied to the analysis of ductile fracture. The main feature is that, with this method, it is not necessary to define a critical value for the damage variable, i.e. the critical void volume fraction at crack initiation. In this sense, this method is similar to that of Rousselier. However, after the initial void volume fraction is selected, the void nucleation parameter(s), which is very difficult to monitor in practice, can be numerically fitted by comparing the predictions with experimental results. Two strain-controlled void nucleation models have been studied and applications made to determine the nucleation parameters for the two nucleation models. Despite the very different intensity distributions, it was interesting to find that the two models with identical A_0 and f_N give very similar predictions. Furthermore, several critical issues have been studied and it has been found that both mesh size and f_F will affect the post initiation load-displacement behaviour. In general, though various approximations have been made in the formulations, reasonably good agreement between the predicted and experimental behaviour indicates that the current method is reasonably accurate and simple to use in the analysis of ductile fracture. The parameters calibrated in this study have been applied to the fracture behaviour of welded joints and very good results have been obtained.

Acknowledgement—The first author would like to thank the Ministry of Education of Finland for financial support.

REFERENCES

1. G. Rousselier (1987) Ductile fracture models and their potential in local approach of fracture. *Nucl. Engng Design* **105,** 97–111.
2. J. Delmotte, J. M. Roelandt and A. Abisror (1990) A numerical analysis to assess ductile tearing in thin plates using local approach—application to *R* curve simulation. In: *Proceedings of the 5th International Conference on Numerical Methods in Fracture Mechanics* (Edited by A. R. Luxmoore and D. R. J. Owen), Pineridge Press, pp. 631–643.
3. B. A. Bilby, I. C. Howard and Z. H. Li (1992) Prediction of the first spinning cylinder test using ductile damage theory, *Fatigue Fract. Engng Mater. Struct.* **16,** 1–20.
4. C. L. Chow and J. Wang (1988) A finite element analysis of continuum damage mechanics for ductile fracture. *Int. J. Fract.* **38,** 83–102.
5. Y. d'Escatha and J. C. Devaux (1979) *Numerical study of initiation, stable crack growth and maximum load, with a ductile fracture criterion based on the growth of holes.* ASTM STP 668, pp. 229–248.
6. A. L. Gurson (1975) Plastic flow and fracture behaviour of ductile materials incorporating void nucleation, growth, and interaction. Ph.D Dissertation, Brown University.
7. A. L. Gurson (1977) Continuum theory of ductile rupture by void nucleation and growth: part I—yield criteria and flow rules for porous ductile media. *J. Engng Mater. Tech.* **99,** 2–15.
8. V. Tvergaard (1981) Influence of voids on shear band instabilities under plane strain conditions, *Int. J. Fract.* **17,** 389–407.
9. V. Tvergaard (1982) On localization in ductile materials containing spherical voids. *Int. J. Fract.* **18,** 237–252.
10. V. Tvergaard and A. Needleman (1984) Analysis of the cup-cone fracture in a round tensile bar. *Acta Metall.* **32,** 157–169.
11. A. Needleman and V. Tvergaard (1987) An analysis of ductile rupture modes at a crack tip. *J. Mech. Phys. Solids* **35,** 151–183.

12. N. Aravas and R. M. McMeeking (1985) Microvoid growth and failure in the ligament between a hole and a blunt crack tip. *Int. J. Fract.* **29,** 21–38.
13. R. Narasimhan, A. J. Rosakis and B. Moran (1992) A three-dimensional numerical investigation of fracture initiation by ductile mechanisms in a 4340 steel. *Int. J. Fract.* **56,** 1–24.
14. D. Z. Sun, D. Siegele, B. Voss and W. Schmitt (1989) Application of local damage models to the numerical analysis of ductile rupture. *Fatigue Fract. Engng Mater. Struct.* **12,** 210–212.
15. D.Z. Sun, B. Voss and W. Schmitt (1991) Numerical prediction of ductile fracture resistance behaviour based on micromechanical models. *Defect Assessment in Components—Fundamentals and Applications.* ESIS/EGF9 (Edited by J. G. Blauel and K.-H. Schwalbe), pp. 447–458. Mechanical Engineering Publications, London.
16. P. F. Thomason (1990) *Ductile Fracture of Metals.* Pergamon Press, Oxford.
17. P. F. Thomason (1985) Ductile fracture and the stability of incompressible plasticity in the presence of microvoids. *Acta Metall.* **29,** 763–777.
18. P. F. Thomason (1985) A three-dimensional model for ductile fracture by the growth and coalescence of microvoids. *Acta Metall.* **33,** 1087–1095.
19. Z. L. Zhang and E. Niemi, A new failure criterion for the Gurson–Tvergaard dilational constitutive model. Submitted to *Int. J. of Fract.*
20. J. Gurland (1972) Observations on the fracture of cementite particles in a spheroidized 1.05%C steel deformed at room temperature. *Acta Metall.* **20,** 735–741.
21. C. C. Chu and A. Needleman (1980) Void nucleation effects in biaxially stretched sheets, *J. Engng Mater. Tech.* **102,** 249–256.
22. Z. L. Zhang (1994) A micro-mechanical model based local approach methodology for the ductile fracture of welded T-joints. Ph.D Dissertation, Lappeenranta University of Technology.
23. Z. L. Zhang and E. Niemi, Studies on the ductility predictions by different local failure criteria. *Engng Fract. Mech.*, in press.
24. J. Koplik and A. Needleman (1988) Void growth and coalescence in porous plastic solids, *Int. J. Solids Struct.* **24,** 835–853.
25. J. R. Rice and D. M. Tracey (1969) On the ductile enlargement of voids in triaxial stress fields. *J. Mech. Phys. Solids* **17,** 201–207.
26. Z. L. Zhang, On the accuracies of numerical integration algorithms for Gurson–Tvergaard pressure-dependent elastoplastic constitutive models. Submitted to *Computer Meth. Appl. Mech. Engng.*
27. Z. L. Zhang and E. Niemi, A class of generalized mid-point algorithms for Gurson–Tvergaard material model. Accepted by *Int. J. Numer. Meth. Engng.*
28. R. Soininen, E. Niemi and Z. L. Zhang, Studies of the fracture behaviour of RHS K-joints at low temperatures. To be published.
29. R. Hill (1971) *The Mathematical Theory of Plasticity.* Oxford University Press.
30. R. Batisse, M. Bethmont, G. Devesa and G. Rousslier (1987) Ductile fracture of A508 CL3 steel in relation with inclusion content: The benefit of the local approach of fracture and continuum damage mechanics. *Nulc. Engng Design* **105,** 113–120.
31. A. G. Franklin (1969) Comparison between a quantitative microscopic and chemical methods for assessment on non-metallic inclusions. *J. Iron Steel Inst.* **207,** 181–186.